Kasahara, J., Stephen, R.A., Acton, G.D., and Frey, F.A. (Eds.)
Proceedings of the Ocean Drilling Program, Scientific Results Volume 200

4. Cenozoic Radiolaria Biostratigraphy of Hole 1223A in the North Pacific: ODP Leg 200[1]

Irina M. Popova-Goll[2] and Robert M. Goll[2]

ABSTRACT

Among the groups of oceanic microfossils, only Radiolaria occur in abundances and preservation states sufficient to provide biostratigraphic control for restricted intervals within sediments recovered in Hole 1223A. The distribution of these microfossils has been divided into four major intervals, A–D. Radiolaria distribution Interval A occupies the depth range 0–3.0 meters below seafloor (mbsf), where the abundance of specimens is very low and preservation is poor. Radiolaria distribution Interval B occupies the depth range 3.02–7.1 mbsf. Radiolaria in Interval B are locally rare to abundant and well preserved, and assemblages range in age from pure early Eocene to early Eocene admixed with late Neogene taxa. Radiolaria distribution Interval C occupies the depth range 7.1–36.99 mbsf and is characterized by sediments either barren of microfossils or containing extremely rare early Eocene specimens. Radiolaria distribution Interval D occupies the depth range 36.99–38.7 mbsf (base of the recovered sedimentary section), where early Eocene Radiolaria are present in rare to common frequencies, but opal-A to opal-CT recrystallization has degraded the preservation state.

The late Neogene assemblage of Radiolaria distribution Interval B is dated at 1.55–2.0 Ma, based on occurrences of *Eucyrtidium matuyamai, Lamprocyclas heteroporos*, and *Theocorythium trachelium trachelium*. The early Eocene assemblage of Radiolaria distribution Intervals B and D is somewhat problematically assigned to the *Buryella clinata* Zone.

[1] Popova-Goll, I.M., and Goll, R.M., 2006. Cenozoic Radiolaria biostratigraphy of Hole 1223A in the North Pacific: ODP Leg 200. *In* Kasahara, J., Stephen, R.A., Acton, G.D., and Frey, F.A. (Eds.), *Proc. ODP, Sci. Results,* 200, 1–26 [Online]. Available from World Wide Web: <http://www-odp.tamu.edu/publications/200_SR/VOLUME/CHAPTERS/007.PDF>. [Cited YYYY-MM-DD]
[2] Integrated Ocean Drilling Program, Texas A&M University, College Station Texas 77845-9547, USA.
Correspondence author: **goll_i@iodp.tamu.edu**

Initial receipt: 8 June 2004
Acceptance: 28 March 2006
Web publication: 17 July 2006
Ms 200SR-007

INTRODUCTION

The primary objectives at Ocean Drilling Program (ODP) Site 1223 were to determine the depositional history, timing, thickness, and hazards associated with the Nuuanu landslide (Stephen, Kasahara, Acton, et al., 2003), which originated on the northeast flank of Koolau volcano and removed 3000–4000 km² of the island of Oahu (Satake et al., 2002). The resulting debris avalanche swept enormous blocks of rock and associated turbidites north across a wide area of the seafloor. Site 1223 is located in the debris field produced by the Nuuanu and neighboring Wailau landslides (Fig. F1), near the crest of the Hawaiian arch ~260 km northeast of Oahu (22°58.409′N, 155°39.2590′W; water depth = 4235.1 m) (see table T5 in Shipboard Scientific Party, 2003a, and fig. F1 in Shipboard Scientific Party, 2003b). Originally scheduled for continuous coring of the upper 100 m of the sediment column, drilling terminated in Hole 1223A at only 41 meters below seafloor (mbsf) because of time constraints. An unexpected and pronounced increase in sedimentary hardness at 12.7 mbsf resulted in a bit change below Core 200-1223A-2H. Consequently, drilling rates were slower than anticipated, and only 23.54 m of sediments was recovered in six cores.

The sediments recovered in these six cores from Hole 1223A were divided into 14 lithologic units (Shipboard Scientific Party, 2003b, pp. 8–14 and fig. F2). Cores 200-1223A-1H and 2H include lithologic Units 1–4 and consist of eight stacked, unconsolidated volcaniclastic turbidites, each >10 cm thick, as well as an unreported number of turbidites of lesser thickness. Cores 200-1223A-3X to 6X include lithologic Units 5–14. The principal components of this lower section are two thick sandstone beds (lithologic Unit 5 and Subunit 11a), described as crystal vitric tuffs separated and underlain by weakly consolidated, very fine grained volcaniclastic claystones and siltstones.

The age of the Nuuanu landslide has been inferred on the basis of isotopic and paleomagnetic analyses. Normark et al. (1993) proposed an age range of 1.4–2.6 Ma for the landslide based on previous K-Ar determinations of Koolau lavas. Paleomagnetic data from piston cores from the debris field led Kanamatsu and Herrero-Bervera (2002) to conclude that the landslide occurred at 1.77–2.58 Ma. Herrero-Bervera et al. (2002) derived an age range of 1.8–2.1 Ma for this event. Stephens, Kasahara, Acton, et al. (2003) interpreted the paleomagnetic stratigraphy of Hole 1223A to yield a basal age of <2.58 Ma. The present study was undertaken to provide an independent determination of the age of Hole 1223A sediments based on biostratigraphy.

F1. Site 1223 location, p. 19.

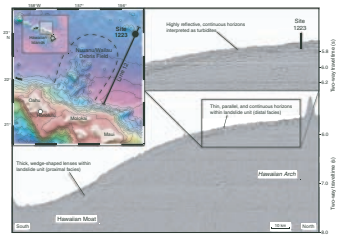

METHODS

A total of 99 smear slides were made from Hole 1223A sediments in lithologic Units 1–3, 6, 7, 9, and 12–14 (Table T1). These slides were made of average sedimentary thickness and mounted on 22 mm × 40 mm coverslips using Norland optical adhesive. Additionally, six smear slides made by the Leg 200 shipboard scientific party from lithologic Units 3, 4, and 10 were included in our study. These slides were examined for microfossil content as well as to qualitatively estimate the concentration of clastic grains in the sediments. A simple technique was used to obtain a quantitative estimate of the frequency of Radiolaria by counting the number of specimens (whole and broken fragments) en-

T1. Smear slide descriptions, p. 24.

countered on one lengthwise pass across the coverslip under the compound microscope with a 10× objective. This count was multiplied by a factor necessary to arrive at a frequency in terms of specimens per square centimeter of smear slide. The results of this investigation are shown Figure F2 and Table T1.

On the basis of our smear slide investigation, 31 samples of bulk sediments were selected for micropaleontological examination. These samples were placed in centrifuge tubes and immersed in a 50% saturated solution of sodium sulfate. A series of eight freeze-thaw cycles dispersed the clays, followed by wet sieving using a 44-µm sieve. Residues were mounted under 22 mm × 40 mm coverslips with Norland optical adhesive. The abundance of individual taxa observed on these slides is recorded in Table T2 as follows:

T = trace (single specimen per slide).
R = rare (2–5 specimens per slide).
C = common (6–10 specimens per slide).
A = abundant (>10 specimens per slide).

These abundance estimates have very limited precision and significance because the mounted residues are diluted by highly variable concentrations of volcanic glass and other clastic grains.

OCCURRENCES

Closely spaced smear slides were examined from selected intervals of Hole 1223A sediments in order to determine the distribution and general characteristics of microfossils in these sediments in anticipation of our routine micropaleontological preparation procedure. The results of these observations are shown in Table T1, which includes a brief description of the microfossils we observed, our estimate of the frequency of Radiolaria in each sample, and a qualitative observation of the concentration of silt-sized clastic grains. High to very high concentrations of clastic grains are interpreted to indicate the basal intervals of turbidite beds. Low to moderate concentrations of clastic grains indicate the fining-upward portions of turbidites or purely pelagic intervals interbedded within stacked turbidites.

With the exception of single specimens of small foraminifers at 0.6, 5.3, and 5.4 mbsf, Radiolaria are the only microfossils observed in these smear slides. Stephens, Kasahara, Acton, et al. (2003) reported occurrences of sponge spicules in lithologic Unit 1, but we found no evidence of these fossils in our slides. We observed abundant occurrences of fine tabulate crystals at 1.9 and 2.0 mbsf, which coincide approximately with the depths given by Stephens, Kasahara, Acton, et al. (2003) for sponge spicules, but the crystals we observed lack the characteristic morphology of sponge spicules. Similar occurrences were observed in the interval 7.33–7.81 and 38.69–38.83 mbsf. These crystals may be dispersed opal-CT blades or zeolitic minerals.

In general, the distribution of Radiolaria in Hole 1223A sediments can be divided into four intervals (A–D). Interval A comprises the depth range 0–3 mbsf and occupies the upper half of lithologic Unit 1 (Sections 200-1223A-IH-1 through 2). Of the 32 smear slides, 25 are barren of microfossils. Seven samples contain small fragments of skeletal lattice in frequencies of 13–26 specimens/cm². Many of these specimens are encrusted with pyrite or manganese, which is common for red clays.

F2. Smear slide and strewn slide samples, p. 20.

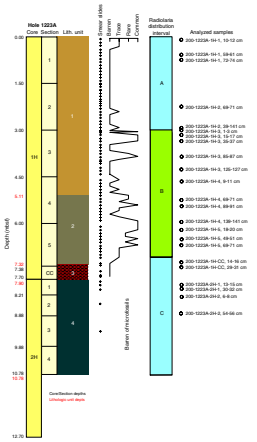

T2. Biostratigraphic distribution, p. 26.

The high frequency of lattice breakage is consistent with turbidite transport. These occurrences were found in pelagic clays from 0.18 to 0.6 mbsf (Subinterval A1) and in the turbidite beds from 2.07 to 2.4 mbsf (Subinterval A2). Opal-CT pseudomorphs or casts of Radiolaria are locally abundant throughout Interval A.

Both preservation state and frequencies of occurrence improve markedly in Interval B, which occupies the depth range 3.02–7.1 mbsf and includes the lower half of lithologic Unit 1 and essentially all of lithologic Unit 2. Radiolaria are present as larger fragments or whole specimens, but occurrences are sporadic. In Interval B, 16 of the 41 smear slides are barren of microfossils. The distribution of Radiolaria in Interval B has been divided into four subintervals (B1–B4), which may be associated with either clastic-rich or clay-rich sediments. Subinterval B1 occupies the depth range 3.02–3.36 mbsf and includes both clay and silt beds. The sample at 3.16 mbsf contains the second highest frequency of Radiolaria (460 specimens/cm^2) and can be described as Radiolaria ooze. Subinterval B2 occupies the depth range 3.76–3.96 mbsf and has Radiolaria frequencies of 40–171 specimens/cm^2. The clay-rich sediments underlying Subintervals B1 and B2 are barren of microfossils. Subintervals B3 and B4 occur in basal lithologic Unit 1 and upper to middle lithologic Unit 2. These two subintervals are separated by a barren interval 40 cm thick. The top of Subinterval B3 spans the top of lithologic Unit 2, from 5.1 to 5.4 mbsf. Only modest frequencies of Radiolaria (13–118 specimens/cm^2) occur in this subinterval. Subinterval B4 occupies the depth range 5.8–7.1 mbsf. Radiolaria frequencies are quite variable but range up to the highest frequency observed in Hole 1223A sediments (945 specimens/cm^2 at 6.7 mbsf). This latter sample is remarkable for the abundance and excellence of preservation of Radiolaria in association with very high concentrations of volcaniclastic grains.

Microfossils were not observed in Interval C, which includes lithologic Units 3–11 and occupies the depth range 7.1–36.99 mbsf. We did not examine the black sands and vitric tuffs of lithologic Units 5, 8, and 11.

Interval D occupies the depth range 36.99–38.7 mbsf and includes the volcaniclastic silty claystones and clayey siltstones (lithologic Units 12–14) immediately underlying the palagonitized vitric tuff of lithologic Unit 11. Very poorly preserved Radiolaria in frequencies of 13–131 specimens/cm^2 are consistently present in these sediments. Opal-CT recrystallization has occurred through this interval. Identifiable specimens of Radiolaria are sparsely present in the upper portion of this interval, but preservation state degrades with depth.

BIOSTRATIGRAPHY

The results of our biostratigraphic examinations are presented in Table **T2,** which includes columns for the lithologic units (Stephens, Kasahara, Acton, et al., 2003) to which the sample depth was assigned along with the Radiolaria occurrence interval/subinterval assignment as described above.

The most noteworthy observation of this investigation is the presence of well-preserved and rare to abundant Radiolaria in the six samples from Subintervals B3 and B4. The 45 taxa that collectively constitute this assemblage are Paleogene in age. Rare to common and consistent occurrences of *Buryella clinata* in these subintervals, as well

as frequent trace to rare occurrences in the overlying and underlying sections, indicate an assignment to the uppermost lower Eocene *Buryella clinata* Zone. The only indication of a possible lower zonal assignment is the observation of a single specimen of *Bekoma bidartensis* in the sample at 4.59 mbsf, which is positioned above Subinterval B3 and probably reworked. The *B. clinata* Biochron has an age range of ~50.3–52.85 Ma (Sanfilippo and Nigrini, 1998). This zonal assignment, however, is not without ambiguities. Sanfilippo and Blome (2001) reported *Thyrsocyrtis rhizodon* occurring first at the base of the overlying lower middle Eocene *Phormocyrtis striata striata* Zone. This species has trace to common occurrences in four of the six samples from Subintervals B3–B4. Moreover, one whole specimen we identified as *Theocorys anaclasta* was observed in the sample at 6.18 mbsf, and other fragments of specimens tentatively assigned to this species and *Theocorys acroria* were observed at 6.18 and 6.49 mbsf. These occurrences force us to consider that Subintervals B3–B4 may belong to the *P. s. striata* Zone or that the entire assemblage contains mixed representatives of both zones. The *P. s. striata* Biochron has an age range of ~49–50.3 Ma (Sanfilippo and Nigrini, 1998). However, we prefer an assignment to the *B. clinata* Zone for Subintervals B3 and B4.

Taxonomic identifications are much more difficult in the sediments below Subintervals B3 and B4 because of extremely low abundances in Interval C and very poor preservation states in Interval D. Three of the seven samples from Interval C are barren of Radiolaria, and the remaining samples contain only trace or rare occurrences with poor to moderate preservation. Only six taxa were identified in these slides. However, traces of *B. clinata* occur in two of these samples, in association with *P. s. striata* and *Sethocyrtis babylonis*. A total of 19 taxa were identified in the six samples from Interval D, among them *B. clinata* at 37.47 and 37.67 mbsf. In the absence of younger or older index taxa, we tentatively assign Intervals C and D to the *B. clinata* Zone.

Components of the Radiolaria assemblage of Subintervals B3–B4 occur sporadically above Subinterval B3, and trace occurrences of *B. clinata* were observed as high as Subinterval A1. However, the Eocene fauna is admixed with Neogene taxa in the samples above Subinterval B3. Perhaps the most obvious evidence for diachronous faunas in the sediments at 5.19 mbsf is the presence of the collosphaerid, *Siphonosphaera socialis,* and *Acrosphaera spinosa, Collosphaera murrayana*, *Clathrosphaera circumtexta*, and *Otosphaera polymorpha*, which are restricted to sediments no older than Miocene in age. The diversity of the Neogene fauna increases upsection to the top of Interval B, and 40 Neogene taxa were identified. The age of this Neogene fauna is somewhat problematic. *Lychnocanoma nipponica nipponica* has a consistent occurrence in the four samples from Subintervals B1–B2. Morley and Nigrini (1995) reported the last occurrence ages of this species in the North Pacific as 6.25–9.6 Ma. This taxon would indicate that the Neogene Radiolaria assemblage between 3.01 and 3.85 mbsf is late Miocene in age; however, we are suspicious of the biostratigraphic reliability of this species. It is also possible that this Neogene assemblage is a composite of more than one fauna, and we must give greatest consideration to the youngest observed taxa. We conclude that the presence of *Eucyrtidium matuyamai* and *Lamprocyrtis heteroporos* in the sample at 3.15 mbsf are better indications of the age of this Neogene assemblage. Morley and Nigrini (1995) give ages of 1.0 and 2.0 Ma for the last occurrence and first occurrence, respectively, of *E. matuyamai,* using the timescale of Cande and Kent (1992). These authors give an age of 1.79 Ma for the last oc-

currence of *L. heteroporos* in the North Pacific. Based on the overlapping distributions of these two taxa in Hole 1223A, an age of 1.79–2.0 Ma is indicated for the Neogene Radiolaria assemblage in Subinterval B1. This biostratigraphic age estimate is in reasonably good agreement with the assignment of these sediments to Magnetochron C2N by Stephens, Kasahara, Acton, et al. (2003). However, Shackleton et al. (1995a) estimated somewhat different ages for biostratigraphic events based on ODP Leg 138 sites in the eastern equatorial Pacific and employing the timescale of Shackleton et al. (1995b). These authors found the age of 1.61 Ma for the last occurrence of *L. heteroporos* and 1.55 Ma for the first occurrence of *Theocorythium trachelium trachelium*. Although their occurrences are somewhat skewed, the presence these two taxa in Interval B suggests an age range of 1.55–1.61 Ma (Magnetochron C1r2r). Subjective bias in taxonomic identification, differing timescales, and disturbed stratigraphic ordering associated with turbidite sedimentation can account for the modest inconsistencies in this chronostratigraphy. In light of the many uncertainties in dating this material, we conclude that the age of Subintervals B1 and B2 is 1.55–2.0 Ma (late Pliocene to early Pleistocene), and the combined subintervals are assigned to the *E. matuyamai* Zone of Hays (1970).

Determining the age of the sediments in Interval A is very difficult because of the sparse occurrences of Radiolaria in poor preservation states. The more robust lattice construction of Paleogene taxa is favored for preservation over the more delicate Neogene skeletal lattice in sediments where SiO_2 dissolution is pronounced. Thus, *B. clinata* is one of only 13 taxa that could be identified in Interval A, in association with three collosphaerid taxa and *Orocena regalis*. In the absence of index taxa with well-established stratigraphic ranges, we can only assign a late Neogene age to Interval A.

DISCUSSION

Biostratigraphic analyses can provide ages for the fossil contents of sediments that should represent the age of original deposition. For sections interpreted as having undergone secondary transport in the form of mass movement, biostratigraphy can only provide information concerning the minimum age of the sediments immediately underlying the redeposited interval. Thus, the age of the underlying sediment indicates only a maximum age for the redistribution event itself. The early Eocene age of the Radiolaria in Subintervals B3–B4 and the more speculative similar ages for Intervals C–D indicate only a maximum age for a stratigraphic section assumed to have arrived at this location by mass wasting at a much younger age. Biostratigraphic analyses of sediments above and below a turbidite can restrict the time frame of the transport event. Despite the absence of microfossils in our smear slides from lithologic Units 3 and 4, we investigated six samples from this section with the objective of finding enough Radiolaria specimens to further constrain the ages of the turbidites in lithologic Unit 2. However, Radiolaria younger than Eocene were not observed in these samples, with the exception of a trace occurrence of *Euchitonia furcata* in the sample at 8.75 mbsf. The Neogene Radiolaria fauna in Subintervals B1–B2 provide a minimum age of 1.61–1.8 Ma for the turbidites below this interval and a maximum age of 2.0 Ma for the turbidites of Interval A.

The occurrences of Radiolaria observed in the sediments in Hole 1223A are consistent with their presence there as a result of the Nuuanu

landslide. Abundant and well-preserved Eocene Radiolaria have an almost global distribution in pelagic sediments (Baldauf and Barron, 1990), and the presence of this Eocene fauna in sediments derived from the sedimentary apron of Koolau Volcano requires no special explanation; however, the presence of the Neogene fauna at this location in the central gyre of the North Pacific is not easily explained. Siliceous microfossil dissolution proceeds to essential completion in the low-productivity regions of the central gyres of the modern oceans. Possibly, the North Pacific central gyre experienced a brief surge in productivity during the late Pliocene that resulted in elevated delivery rates of siliceous skeletal debris arriving on the seafloor and consequently improved conditions for microfossil preservation. Alternatively, the presence of seafloor sediments containing high concentrations of volcaniclastic components as a result of the Nuuanu landslide may have produced environments where silica dissolution was sufficiently depressed to allow partial preservation of siliceous skeletal debris. This latter explanation, however, is not consistent with the distribution of Radiolaria in Hole 1223A immediately above Subintervals B3–B4, where opal-A preservation is very poor.

Stephens, Kasahara, Acton, et al. (2003) postulated that the two vitric tuffs of lithologic Units 5 and 11 may have resulted from a very large eruption of primitive tholeiite that occurred when a deep magma reservoir was breached during failure of the northeast flank of Koolau Volcano, thus resulting in the giant Nuuanu debris avalanche. The volcaniclastic sand resulting from this eruption and the sediments entrained with it are believed to have been swept north at tremendous speed as a submarine debris flow. These authors suggest that the heat retained within the debris flow caused alteration and induration of the two vitric tuffs. This heat source may have also been responsible for the opal-A to opal-CT alteration of Radiolaria in the claystones and siltstones below the tuffs (Interval D). Garcia et al. (2006) present evidence against the hot debris flow model and argue that the tuffs are more correctly described as sandstones; however, we observe that the degree of opal-CT recrystallization in Interval D appears to increase with depth. Consequently, the heat source responsible for induration of the sediments below Core 200-1223A-2H and opal-CT recrystallization of Interval D may be located in the sediment column below 41 mbsf at Site 1223.

Similarities between the Eocene Radiolaria assemblages preserved in Hole 1223A sediments suggest that the entire section was derived from the same source location. The mixed ages of the Radiolaria assemblage above Subinterval B3 may indicate that the source of these younger turbidites was shifting to a different location on Koolau, where late Pliocene sediments were available for transport and redeposition.

The improved state of preservation of the Radiolaria in Interval B is in marked contrast to the highly fragmented condition of the skeletal lattice observed in Interval A. We commented above on the unusual nature of the sediment at 6.7 mbsf, where abundant and well-preserved Radiolaria are associated with a very high concentration of volcaniclastic grains. Whereas the condition of the Radiolaria in Interval A is consistent with turbidite transport over long distances, the good to very good preservation of specimens in Subintervals B3–B4 suggests a less abrasive depositional process. Perhaps Subintervals B3–B4 arrived at Site 1223 as an intact unit within the Koolau debris avalanche. Alternatively, Subintervals B3–B4 may have been emplaced as a single, local slump derived from the one of the numerous blocks and seamounts of

the Nuuanu-Wailau debris field. Intermittently abundant occurrences of tabulate crystals suspected of being opal-CT blades in the sediments of Intervals A and B may be further evidence of local weathering and redeposition of sedimentary constituents derived from outcrops of Interval D claystones and siltstones.

Mixed Radiolaria assemblages composed of faunas with ages similar to those of Hole 1223A occur elsewhere in the central North Pacific. At Deep Sea Drilling Project (DSDP) Site 40 (~1700 km east-southeast of Site 1223), the upper 10 m of the stratigraphic section consists of zeolitic red clay containing a Radiolaria assemblage predominantly comprising Eocene taxa with minor late Neogene constituents. This interval is immediately underlain by 143 m of Eocene Radiolaria ooze (McManus et al., 1970). Unfortunately, a detailed biostratigraphic analysis of the upper portion of this hole is not available. Benthic burrowers may account for the fossil admixture at Site 40, but the vast preponderance of the Eocene admixed constituents is troubling. At other localities where burrowing by benthic organisms is obvious, the older and deeper fauna that has been reworked up through the sediment column represents only a minor percentage of the total fossil assemblage. Inexplicably, the upper sediments at Site 40 contain about 95% Eocene taxa admixed with minor concentrations of Pleistocene species. Sedimentary reworking by burrowers is an even less probable explanation for the mixed assemblage present in Hole 1223A, where the immediately underlying sediments are barren.

Important similarities and distinctions exist between the distributions of Radiolaria in the section recovered at Site 1223 and those of ODP Leg 136 Sites 842 and 843, which are located 320 km west of the island of Hawaii. The stratigraphic sections at Sites 842 and 1223 both include intervals ~1 m thick containing mixed late Neogene and Eocene Radiolaria within stacked turbidites. In the Leg 136 recovery, these mixed faunas are restricted to three ash layers in the 7.5–9.6 mbsf interval of Hole 842A (Garcia and Hull, 1994). These ash beds are interspersed in a succession of brown clay and clayey silts containing common to abundant, exclusively Neogene Radiolaria variously dated as Quaternary (Hull, 1993), Pleistocene (Garcia and Hull, 1994), or assigned to the lower Pleistocene *Amphirhopalum ypsilon* Zone (Hull, 1993). More precise age determinations for this assemblage is precluded by the absence of critical index taxa. The magnetostratigraphic record of Holes 842A and 842B suggests that the ash beds were deposited during early Magnetochron C1r2r (Helsley, 1993; Garcia and Hull, 1994). This succession at Site 842, containing an undiluted Neogene Radiolaria assemblage, is replaced by the largely barren turbidites of Interval A in Hole 1223A. Moreover, admixture of Neogene and Eocene faunas is not restricted to volcaniclastic sediments in Interval B of Hole 1223A, and the recovery from Holes 842 and 843 lack beds containing purely Eocene Radiolaria, as represented in Subinterval B2. The black, indurated claystones cemented with opal-CT of Cores 136-842B-3H and 4H (Shipboard Scientific Party, 1992) may be correlative with lithologic Units 5 and 11 of Site 1223.

CONCLUSIONS

Biostratigraphic analyses might have provided a maximum age estimate for the Nuulau landslide had we found adequately preserved fossils in the sedimentary section below the landslide section. However,

Hole 1223A may not have penetrated subslide sediments, and the Eocene Radiolaria assemblage observed in Intervals B and D indicate only a maximum age for timing of the turbidite events recovered in the sediment column above 41 mbsf. In this case, the maximum age has little value, but the Neogene Radiolaria fauna in Subintervals B1–B2 provide a minimum age of 1.8 Ma for the turbidites below 3 mbsf and a maximum age of 2.0 Ma for the turbidites of Interval A. We have made extensive examinations of our prepared samples from Interval A in order to obtain biostratigraphic age control, but the paucity of microfossils, including Radiolaria, precludes this objective.

We speculate on the basis of inconclusive evidence that the heat source responsible for induration of the section below Core 200-1223A-2H and opal-CT recrystallization in Interval D may be located in the section below 41 mbsf at Site 1223. Furthermore, we suggest that volcaniclastic-rich sediments of lithologic Unit 2 may represent a local cohesive slump rather than stacked distal turbidites.

ACKNOWLEDGMENTS

Permission to sample and examine cores was provided by the Ocean Drilling Program (ODP). ODP is sponsored by the U.S. National Science Foundation (NSF) and participating countries under management of Joint Oceanographic Institutions (JOI), Inc. A contribution toward laboratory processing costs was provided from a JOI/U.S. Science Support Program grant to Dr. M. Garcia.

REFERENCES

Bailey, J.W., 1856. Notice of microscopic forms found in the soundings of the Sea of Kamtschatka—with a plate. *Am. J. Sci.,* 22:1–6.

Baldauf, J.G., and Barron, J.A., 1990. Evolution of biosiliceous sedimentation patterns—Eocene through Quaternary: paleoceanographic response to polar cooling. *In* Bleil, U., and Thiede, J. (Eds.), *Geological History of the Polar Oceans: Arctic Versus Antarctic:* Dordrecht (Kluwer Academic), 575–607.

Benson, R.N., 1966. Recent Radiolaria from the Gulf of California [Ph.D. dissert.]. Univ. of Minnesota, Minneapolis.

Bjørklund, K.R., 1976. Radiolaria from the Norwegian Sea, Leg 38 of the Deep Sea Drilling Project. *In* Talwani, M., Udintsev, G., et al., *Init. Repts. DSDP,* 38: Washington (U.S. Govt. Printing Office), 1101–1168.

Bjørklund, K.R., and Goll, R.M., 1979. Internal skeletal structures of *Collosphaera* and *Trisolenia:* a case of repetitive evolution in the Collosphaeridae (Radiolaria). *J. Paleontol.,* 53:1293–1326.

Borgert, A., 1901. Die nordischen Tripyleen-Arten. *Nord. Plankton,* 15:1–52.

Brandt, R., 1935. Die Mikropalaeontologie des Heiligenhafener, Kieseltones (Ober-Eozan) Radiolarien, Systematik. *In* Wetzel, E.O. (Ed.), *Jahresber. Niedersaechs. Geol. Ver.,* 27:48–59.

Cande, S.C., and Kent, D.V., 1992. A new geomagnetic polarity time scale for the Late Cretaceous and Cenozoic. *J. Geophys. Res.,* 97(10):13917–13951.

Caulet, J.-P., 1979. Les depots a radiolaires d'age Pliocene superieur a Pleistocene dans l'ocean Indien central: nouvelle zonation biostratigraphique (Radiolarian upper Pliocene–Pleistocene deposits in the central Indian Ocean; new biostratigraphic zonation). *Mem. Mus. Nat. Hist., Nat. Ser. C (Paris),* 43:119–141.

Chen, P.-H., 1975. Some new Tertiary radiolaria from Antarctic deep-sea sediments. *Micropaleontology,* 20:480–492.

Clark, B.L., and Campbell, A.S., 1942. Eocene radiolarian faunas from the Mt. Diablo area, California. *Spec. Pap.—Geol. Soc. Am.,* 39:1–112.

Dreyer, F., 1889. Morphologische Radiolarienstudien. 1. Die Pylombildungen in vergleichend-anatomischer und entwicklungsgeschichtlicher Beziehung bei Radiolarien und bei Protisten überhaupt, nebst System und Beschreibung neuer und der bis jetzt bekannten pylomatischen Spumellarien. *Jena. Z. Naturwiss.,* 23:1–138.

Ehrenberg, C.G., 1844. Über 2 neue Lager von Gebirgsmassen aus Infusorien als Meeres-Absatz in Nord-Amerika und eine Vergleichung derselben mit den organischen Kreide-Gebilden in Europa und Afrika. *K. Preuss. Akad. Wiss. Berlin, Ber.,* 57–97.

Ehrenberg, C.G., 1847. Über die mikroskopischen kieselschaligen Polycystinen als mächtige Gebirgsmasse von Barbados und über das Verhältniss deraus mehr als 300 neuen Arten bestehenden ganz eigenthümlichen Formengruppe jener Felsmasse zu den jetzt lebenden Thieren und zur Kreidebildung. Eine neue Anregung zur Erforschung des Erdlebens. *K. Preuss. Akad. Wiss. Berlin, Ber.,* Jahre 1847:40–60.

Ehrenberg, C.G., 1854. *Mikrogeologie: Das Erden und Felsen schaffende Wirken des unsichtbar kleinen selbständigen Lebens auf der Erde:* Leipzig (Leopold Voss).

Ehrenberg, C.G., 1860. Über den Tiefgründ des stillen Oceans zwischen Californien und den Sandwich-Inseln aus bis 15600' Tiefe nach Lieutenant Brooke. *K. Preuss. Akad. Wiss. Berlin, Monatsber.,* 1860:819–833.

Ehrenberg, C.G., 1862. Über die Tiefgrund-Verhältnisse des Oceans am Eingange der Davisstrasse und bei Island. *K. Preuss. Akad. Wiss. Berlin, Monatsberichte,* 1862:131–399.

Ehrenberg, C.G., 1872a. Mikrogeologische Studien als Zusammenfassung der Beobachtungen des kleinsten Lebens der Meeres-Tiefgrunde aller Zonen und dessen geologischen Einfluss. *K. Preuss. Akad. Wiss. Berlin, Monatsberichte,* 1872:265–322.

Ehrenberg, C.G., 1872b. Mikrogeologische Studien über das kleinste Leben der Meeres-Tiefgrunde aller Zonen und dessen geologischen Einfluss. *Abh. K. Akad. Wiss. Berlin,* 1872:131–399.

Ehrenberg, C.G., 1873. Grössere Felsproben des Polycystinen-Mergels von Barbados mit weiteren Erläuterungen. *K. Preuss. Akad. Wiss. Berlin, Monatsberichte,* 1873:213–263.

Ehrenberg, C.G., 1875. Fortsetzung der mikrogeologischen Studien als Gesammt-Uebersicht der mikroskopischen Paläontologie gleichartig analysirter Gebirgsarten der Erde, mit specieller Rücksicht auf den Polycystinen-Mergel von Barbados. *Abh. K. Akad. Wiss. Berlin,* 1875:1–225.

Foreman, H.P., 1973. Radiolaria from DSDP Leg 20. *In* Heezen, B.C., MacGregor, I.D., et al., *Init. Repts. DSDP,* 20: Washington (U.S. Govt. Printing Office), 249–305.

Garcia, M.O., and Hull, D.M., 1994. Turbidites from giant Hawaiian landslides; results from Ocean Drilling Program Site 842. *Geology,* 22:159–162. **doi:10.1130/0091-7613(1994)022<0159:TFGHLR>2.3.CO;2**

Garcia, M.O., Sherman, S.B., Moore, G.F., Goll, R., Popova-Goll, I., Natland, J.H., and Acton, G., 2006. Frequent landslides from Koolau Volcano: results from ODP Site 1223. *J. Volcanol. Geotherm. Res.,* 151(1–3):251–268. **doi:10.1016/j.jvolgeores.2005.07.035**

Goll, R.M., 1968. Classification and phylogeny of Cenozoic Trissocyclidae (Radiolaria) in the Pacific and Caribbean basins, Part I. *J. Paleontol.,* 42(6):1409–1432.

Goll, R.M., 1969. Classification and phylogeny of Cenozoic Trissocyclidae (Radiolaria) in the Pacific and Caribbean basins, Part II. *J. Paleontol.,* 43(2):322–339.

Goll, R.M., 1972. Systematics of eight *Tholospyris* taxa (Trissocyclidae, radiolaria). *Micropaleontology,* 18:443–475.

Goll, R.M., 1976. Morphological intergradation between modern populations of *Lophospyris* and *Phormospyris* (Trissocyclidae, Radiolaria). *Micropaleontology,* 22(4):379–418.

Goll, R.M., 1979. The Neogene evolution of *Zygocircus, Neosemantis* and *Callimitra:* their bearing on nassellarian classification. A revision of the Plagiacanthoidea. *Micropaleontology,* 25(4):365–396.

Haeckel, E., 1861. Abbildungen und diagnosen neuer gattungen und arten von lebenden radiolarien des Mittelmeeres. *Monatsber. Königlichen Akad. Wiss. Berlin,* 834–845.

Haeckel, E., 1881. Entwurf eines Radiolarien-Systems auf Grund von Studien der Challenger-Radiolarien (Basis for a radiolarian classification from the study of Radiolaria of the Challenger collection). *Jena. Z. Med. Naturwiss.,* 15 (Vol. 8, Pt. 3):418–472.

Haeckel, E., 1887. Report on the radiolaria collected by H.M.S. *Challenger* during the years 1873–1876. *Rep. Sci. Results Voy. H.M.S.* Challenger, *1873–1876, Zool.,* 18:1–1803.

Harting, P., 1863. Bijdrage tot de kennis der mikroskopische faune en flora van de Banda-Zee [Contribution to the knowledge of microscopic fauna and flora from the Banda Sea]. *K. Nederl. Akad. Wetensch., Verhand.,* 10:1–34.

Hays, J.D., 1965. Radiolaria and late Tertiary and Quaternary history of Antarctic seas. *In* Llano, G.A. (Ed.), *Biology of the Antarctic Seas II.* Antarct. Res. Ser., 5:125–184.

Hays, J.D., 1970. Stratigraphy and evolutionary trends of radiolaria in North Pacific deep sea sediments. *In* Hays, J.D. (Ed.), *Geological Investigations of the North Pacific.* Mem.—Geol. Soc. Am., 126:185–218.

Helsley, C.E., 1993. Paleomagnetic results from Leg 136. *In* Wilkens, R.H., Firth, J., Bender, J., et al., *Proc. ODP, Sci. Results,* 136: College Station, TX (Ocean Drilling Program), 45–50.

Herrero-Bervera, E., Cañon-Tapia, E., Walker, G.P.L., Guerrero-Garcia, J.C., 2002. The Nuuanu and Wailau giant landslides: insights from paleomagnetic and anisotropy of magnetic susceptibility (AMS) studies. *Phys. Earth Planet. Inter.,* 129:83–98. **doi:10.1016/S0031-9201(01)00238-2**

Hertwig, R., 1879. Der Organismus der Radiolarien. *Jenaische Denkshr.,* 2:129–277.
Hollis, C.J., 2002. Biostratigraphy and paleoceanographic significance of Paleocene radiolarians from offshore eastern New Zealand. *Mar. Micropaleontol.,* 46:265–316. **doi:10.1016/S0377-8398(02)00066-X**
Hull, D.M., 1993. Quaternary, Eocene, and Cretaceous radiolarians from the Hawaiian Arch, northern equatorial Pacific Ocean. *In* Wilkens, R.H., Firth, J., Bender, J., et al., *Proc. ODP, Sci. Results,* 136: College Station, TX (Ocean Drilling Program), 3–25.
Jörgensen, E., 1905. The protist plankton and the diatoms in bottom samples. *Bergens Mus. Skr.,* 49–151.
Kanamatsu, T., and Herrero-Bervera, E., 2002. Magnetostratigraphy of deep-sea sediments from areas adjacent to the Hawaiian Islands: implications for ages of turbidites derived from submarine landslides. *In* Takahashi, E., Lipman, P.W., Garcia, M.O. Naka, J., and Aramaki, S. (Eds.), *Hawaiian Volcanoes: Deep Underwater Perspectives*. Geophys. Monogr., 128:51–63.
Kling, S.A., 1973. Radiolaria from the eastern North Pacific, Deep Sea Drilling Project, Leg 18. *In* Kulm, L.D., von Huene, R., et al., *Init. Repts. DSDP,* 18: Washington (U.S. Govt. Printing Office), 617–671.
Kozlova, G.E., and Gorbovets, A.N., 1966. Radiolyarii verkhnemelovykh i verkhneeotsenovykh otlozhenii Zapadno-Sibirskoi Nizmennosti [Radiolaria of the Upper Cretaceous and upper Eocene of the west Siberian Lowland]. *Tr. Vses. Neft. Nauchno-Issled. Geologorazved. Inst. (VNIGRI) [Proc. All-Union Pet. Sci. Res. Inst. Geol. Surv. (VNIGRI)],* 248:1–159.
Krasheninnikov, V.A., 1960. Nektorye Radiolyarii Nizhnego i Srednego Eotsens Zapadnogo Predkavkazya [Some radiolarians of the lower and middle Eocene of the westen Caucasus]. *Min. Geol. Okhr. Nedr SSSR, Vses. Nauchno-Issled. Geol. Neft. Inst.,* 16:271–308.
Martin, G.C., 1904. Radiolaria. *In* Clark, W.B., Eastman, C.R., Glenn, L.C., Bagg, R.M., Bassler, R.S., Boyer, C.S., Case, E.C., and Hollick, C.A. (Eds.), *Systematic Paleontology of the Miocene Deposits of Maryland:* Baltimore (Maryland Geol. Surv., Johns Hopkins Press), 447–459.
McManus, D.A., Burns, R.E., von der Borch, C., Goll, R., Milow, E.D., Olsson, R.K., Vallier, T., and Weser, O., 1970. Site 40. *In* McManus, D.A., Burns, R.E., et al. (Eds.), *Init. Repts. DSDP,* 5: (U.S. Government Printing Office). 309–352.
Morley, J.J., and Nigrini, C., 1995. Miocene to Pleistocene radiolarian biostratigraphy of North Pacific Sites 881, 884, 885, 886, and 887. *In* Rea, D.K., Basov, I.A., Scholl, D.W., and Allan, J.F. (Eds.), *Proc. ODP, Sci. Results,* 145: College Station, TX (Ocean Drilling Program), 55–91.
Nigrini, C., 1967. Radiolaria in pelagic sediments from the Indian and Atlantic Oceans. *Bull. Scripps Inst. Oceanogr.,* 11:1–125. [\3-7-94]
Nigrini, C., 1974. Cenozoic Radiolaria from the Arabian Sea, DSDP Leg 23. *In* Davies, T.A., Luyendyk, B.P., et al., *Init. Repts. DSDP,* 26: Washington (U.S. Govt. Printing Office), 1051–1121.
Nigrini, C., 1977. Tropical Cenozoic Artostrobiidae (Radiolaria). *Micropaleontology,* 23:241–269.
Nigrini, C., and Caulet, J.P., 1992. Late Neogene radiolarian assemblages characteristic of Indo-Pacific areas of upwelling. *Micropaleontology,* 38(2):139–164.
Nigrini, C., and Moore, T.C., 1979. *A Guide to Modern Radiolaria.* Spec. Publ.—Cushman Found. Foraminiferal Res., 16.
Normark, W.R., Moore, J.G., and Torresan, M.E., 1993. Giant volcano-related landslides and the development of the Hawaiian Islands. *In* Schwab, W.C., Lee, H.J., Twichell, D.C. (Eds.), *Submarine Landslides: Selected Studies in the U.S. Exclusive Economic Zone*. U.S. Geol. Surv. Bull., 2002:184–196.
Petrushevskaya, M.G., and Kozlova, G.E., 1972. Radiolaria: Leg 14, Deep Sea Drilling Project. *In* Hayes, D.E., Pimm, A.C., et al., *Init. Repts. DSDP,* 14: Washington (U.S. Govt. Printing Office), 495–648.

Renz, G.W., 1974. Radiolaria from Leg 27 of the Deep Sea Drilling Project. *In* Veevers, J.J., Heirtzler, J.R., et al., *Init. Repts. DSDP,* 27: Washington (U.S. Govt. Printing Office), 769–841.

Riedel, W.R., 1953. Mesozoic and late Tertiary Radiolaria of Rotti. *J. Paleontol.,* 27(6):805–813.

Riedel, W.R., and Sanfilippo, A., 1970. Radiolaria, Leg 4, Deep Sea Drilling Project. *In* Bader, R.G., Gerard, R.D., et al., *Init. Repts. DSDP,* 4: Washington (U.S. Govt. Printing Office), 503–575.

Riedel, W.R., and Sanfilippo, A., 1971. Cenozoic Radiolaria from the western tropical Pacific, Leg 7. *In* Winterer, E.L., Riedel, W.R., et al., *Init. Repts. DSDP,* 7 (Pt. 2): Washington (U.S. Govt. Printing Office), 1529–1672.

Riedel, W.R., Sanfilippo, A., and Cita, M.B., 1974. Radiolarians from the stratotype Zanclean (lower Pliocene, Sicily). *Riv. Ital. Paleontol. Stratigr.,* 80:699–734.

Sakai, T., 1980. Radiolarians from Sites 434, 435, and 436, Northwest Pacific, Leg 56, Deep Sea Drilling Project. *In* von Huene, R., Nasu, N., et al., *Init. Repts. DSDP,* 56, 57 (Pt. 2): Washington (U.S. Govt. Printing Office), 695–733.

Sanfilippo, A., and Blome, C.D., 2001. Biostratigraphic implications of mid-latitude Paleocene–Eocene radiolarian faunas from Hole 1051A, Ocean Drilling Program Leg 171B, Blake Nose, western North Atlantic. *In* Kroon, D., Norris, R.D., and Klaus, A. (Eds.), *Western North Atlantic Palaeogene and Cretaceous Palaeoceanography.* Spec. Publ.—Geol. Soc. London, 183:l85–224.

Sanfilippo, A., Burckle, L.H., Martini, E., and Riedel, W.R., 1973. Radiolarians, diatoms, silicoflagellates and calcareous nannofossils in the Mediterranean Neogene. *Micropaleontology,* 19:209–234.

Sanfilippo, A., and Nigrini, C., 1998. Code numbers for Cenozoic low latitude radiolarian biostratigraphic zones and GPTS conversion tables. *Mar. Micropaleontol.,* 33:109–156. **doi:10.1016/S0377-8398(97)00030-3**

Sanfilippo, A., and Riedel, W.R., 1974. Radiolaria from the west-central Indian Ocean and Gulf of Aden, DSDP Leg 24. *In* Fisher, R.L., Bunce, E.T., et al., *Init. Repts. DSDP,* 24: Washington (U.S. Govt. Printing Office), 997–1035.

Sanfilippo, A., and Riedel, W.R., 1979. Radiolaria from the northeastern Atlantic Ocean, DSDP Leg 48. *In* Montadert, L., Roberts, D. G., et al., *Init. Repts., DSDP,* 48: Washington (U.S. Govt. Printing Office), 493–511.

Sanfilippo, A., Westberg-Smith, M.J., and Riedel, W.R., 1985. Cenozoic radiolaria. *In* Bolli, H.M., Saunders, J.B., and Perch-Nielsen, K. (Eds.), *Plankton Stratigraphy:* Cambridge (Cambridge Univ. Press), 631–712.

Satake, K., Smith, J.R., and Shinozaki, K., 2002. Volume estimate and tsunami modeling for the Nuuanu and Wailau landslides. *In* Takahashi, E., Lipman, P.W., Garcia, M.O., Naka, J., and Aramaki, S. (Eds.), *Hawaiian Volcanoes: Deep Underwater Perspectives.* Geophys. Monogr., 128:333–348.

Shackleton, N.J., Baldauf, J.G., Flores, J.-A., Iwai, M., Moore, T.C., Jr., Raffi, I., and Vincent, E., 1995. Biostratigraphic summary for Leg 138. *In* Pisias, N.G., Mayer, L.A., Janecek, T.R., Palmer-Julson, A., and van Andel, T.H. (Eds.), *Proc. ODP, Sci. Results,* 138: College Station, TX (Ocean Drilling Program), 517–536.

Shackleton, N.J., Crowhurst, S., Hagelberg, T., Pisias, N.G., and Schneider, D.A., 1995. A new late Neogene time scale: application to Leg 138 sites. *In* Pisias, N.G., Mayer, L.A., Janecek, T.R., Palmer-Julson, A., and van Andel, T.H. (Eds.), *Proc. ODP, Sci. Results,* 138: College Station, TX (Ocean Drilling Program), 73–101.

Shipboard Scientific Party, 1992. Site 842. *In* Dziewonski, A., Wilkens, R., Firth, J., et al., *Proc. ODP, Init. Repts.,* 136: College Station, TX (Ocean Drilling Program), 37–63.

Shipboard Scientific Party, 2003a. Leg 200 summary. *In* Stephen, R.A., Kasahara, J., Acton, G.D., et al., *Proc. ODP, Init. Repts.,* 200, 1–73 [CD-ROM]. Available from: Ocean Drilling Program, Texas A&M University, College Station TX 77845-9547, USA. [**HTML**]

Shipboard Scientific Party, 2003b. Site 1223. *In* Stephen, R.A., Kasahara, J., Acton, G.D., et al., *Proc. ODP, Init. Repts.,* 200, 1–159 [CD-ROM]. Available from: Ocean Drilling Program, Texas A&M University, College Station TX 77845-9547, USA. [**HTML**]

Stephen, R.A., Kasahara, J., Acton, G.D., et al., 2003. *Proc. ODP, Init. Repts.,* 200 [CD-ROM]. Available from: Ocean Drilling Program, Texas A&M University, College Station TX 77845-9547, USA. [**HTML**]

Van de Paverd, P.J., 1995. Recent polycystine Radiolaria from the Snellius-II expedition [Ph.D. dissert.], Amsterdam.

APPENDIX

Taxa List

The following list of 93 radiolarian taxa identified in Hole 1223A includes a reference to the original description and, optionally, to a recent reference containing emendation, synonymy, or improved illustrations.

Acrosphaera spinosa spinosa (Haeckel) 1861, p. 845; Bjørklund and Goll, 1979, p. 1308, pl. 1, figs. 8, 9.

Acrosphaera murrayana (Haeckel) 1887, pp. 102–103, pl. 8, fig. 4; Benson, 1966, p. 120–121, pl. 2, fig. 3.

Amphicraspedum murrayanum Haeckel, 1887, p. 523, pl. 44, fig. 10.

Amphicraspedum prolixum Sanfilippo and Riedel, 1974, p. 524, pl. 10, figs. 7–11, pl. 28, figs. 3, 4.

Amphirhopalum ypsilon Nigrini, 1967, pl. 35.3, fig. 3.

Anthocyrtidium zanguebaricum Ehrenberg, 1872b, p. 285, pl. 9, fig. 12; Renz, 1974, p. 788, pl. 19, fig. 17.

Bekoma bidartensis Riedel and Sanfilippo, 1971, p. 1592, pl. 7, figs. 1–7; Sanfilippo et al., 1985, p. 667, fig. 13.1a, 13.1b.

Botryostrobus aquilonaris (Bailey) 1856, p. 4, pl. 1, fig. 9; Nigrini, 1977, p. 246, pl. 1, fig. 1.

Botryostrobus auritus-australis (Ehrenberg) Nigrini, 1977, p. 246–247, pl. 1, figs. 2–5.

Buryella clinata Foreman, 1973a, p. 433, pl. 8, figs. 1–3, pl. 9, fig. 19; Sanfilippo et al., 1985, p. 668, fig. 14.1a, 14.1b.

Calocyclas hispida Ehrenberg, 1873, p. 216; 1875, pl. 8, fig. 2; Foreman, 1973, p. 434, pl. 1, figs. 12–15, pl. 9, fig. 18.

Calocyclas sp. cf. *Calocyclas turris* Ehrenberg, 1873, p. 218; 1875, pl. 18, fig. 7; Sanfilippo et al., 1985, p. 669, fig. 15.1a–15.1c.

Calocycloma ampulla Ehrenberg, 1854, pl. 36.15; 1873, p. 22; Sanfilippo et al., 1985, p. 668, fig. 14.5.

Calocycloma castum Haeckel, 1887, p. 1384, pl. 73, fig. 10; Sanfilippo et al., 1985, p. 669, fig. 14.4.

Carpocanopsis cingulata (Riedel and Sanfilippo) 1971, p. 1597, pl. 2G, figs. 17–21, pl. 8, fig. 8; Sanfilippo and Riedel, 1974, p. 531; Sanfilippo et al., 1985, fig. 27.4.

Clathrosphaera circumtexta Haeckel, 1887, p. 118, pl. 8, fig. 6.

Dendrospyris acuta Goll, 1968, p. 1419, pl. 173, figs. 7–9, 12.

Dendrospyris inferispina Goll, 1968, p. 1421, pl. 174, figs. 5–8, 10.

Dendropsyris stabilis Goll, 1968, p. 1422, pl. 173, figs. 16–18, 20.

Dictyophimus pocillum Ehrenberg, 1873, p. 223; 1875, pl. 5, fig. 6; Petrushevskaya and Kozlova, 1972, p. 553, pl. 29, fig. 5.

Dictyoprora amphora Haeckel, 1887, p. 1305, pl. 62, fig. 4; Nigrini, 1977, p. 250, pl. 4, figs. 1, 2.

Dictyoprora urceolus (Haeckel) 1887, p. 1305; Nigrini, 1977, p. 251, pl. 4, figs. 9, 10.

Didymocyrtis avita (Riedel) 1953, p. 808, pl. 84, fig. 7; Sanfilippo et al., 1985, p. 657, fig. 8.8a, 8.8b.

Didymocyrtis tetrathalamus (Haeckel) 1887, p. 378, pl. 40, fig. 3; Sanfilippo et al., 1985, p. 659, figs. 8, 9.

Dorcadospyris argisca (Ehrenberg) 1873, p. 246; 1875, pl. 22, figs. 1, 2, as *Petalospyris*; Goll, 1969, p. 336, pl. 56, figs. 9–11.

Dorcadospyris confluens Ehrenberg, 1873, p. 146; 1875, pl. 22, fig. 5, as *Petalospyris*; Goll, 1969, p. 337, pl. 58, figs. 9–12.

Euchitonia furcata Ehrenberg, 1872a, p. 308; Nigrini and Moore, 1979, pp. S85–S86, pl. 11, fig. 2a, 2b.

Eucoronis challenger (Haeckel) 1881, p. 445; Benson, 1966, pp. 410–412, pl. 28, figs. 2, 3.

Eucyrtidium accuminatum (Ehrenberg) 1844, p. 84; Nigrini and Moore, 1979, p. 61, pl. 24, fig. 3a, 3b.

Eucyrtidium calvertense Martin, 1904, p. 450, pl. 130, fig. 5; Hays, 1970, p. 213, pl. 1, fig. 6.

Eucyrtidium matuyamai Hays, 1970, p. 213, pl. 1, figs. 7–9; Kling, 1973, pl. 4, fig. 17.

Giraffospyris didiceros (Ehrenberg) 1873, pp. 218–219; 1875, pl. 21, fig. 6; Goll, 1969, p. 332, pl. 60, figs. 5–7, 9.

Giraffospyris lata Goll, 1969, p. 334, pl. 58, figs. 22, 24–26.

Gorgospyris schizopodia Haeckel, 1887, p. 1071, pl. 87, fig. 4; Sanfilippo et al., 1973, p. 218, pl. 3, figs. 6, 7.

Heliodiscus hexasteriscus Haeckel, 1887, p. 445, fig. 33.8; Clark and Campbell, 1942, p. 40, pl. 3, figs. 14, 15.

Lamprocyclas maritalis maritalis Haeckel, 1887, p. 1390, pl. 74, figs. 13, 14; Riedel et al., 1974, p. 712, pl. 61, figs. 2, 3.

Lamprocyrtis heteroporos (Hays) 1965, p. 179, pl. 3, fig. 1; Sanfilippo et al., 1985,

fig. 29.3.

Lamprocyrtis neoheteroporos Kling, 1973, p. 639, pl. 5, figs. 17, 18, pl. 15, figs. 4, 5; Sanfilippo et al, 1985, p. 693, fig. 29.2.

Lamptonium fabaeforme chaunothorax Riedel and Sanfilippo, 1970, p. 524, pl. 5, figs. 8, 9; Sanfilippo et al., 1985, p. 673, fig. 18.

Lamptonium fabaeforme fabaeforme (Krasheninnikov) 1960, p. 296, pl. 3, fig. 11; Sanfilippo et al., 1985, p. 674, fig. 18.2.

Lamptonium pennatum Foreman, 1973, p. 436, pl. 6, figs. 3–5, pl. 11, fig. 13; Sanfilippo et al., 1985, p. 674, fig. 18.1.

Lamptonium sanfilippoae Foreman, 1973, p. 436, pl. 6, figs. 15, 16, pl. 11, figs. 16, 17; Sanfilippo et al., 1985, p. 674, fig. 18.5.

Liriospyris reticulata (Ehrenberg) 1872a, p. 307, pl. 10, fig. 19, as *Dictyospyris*; Goll, 1968, pp. 1429–1430, pl. 176, figs. 9, 11, 13, as *Liriosospyris*.

Lithochytris archaea Riedel and Sanfilippo, 1970, p. 528, pl. 9, fig. 7.

Lithopera bacca Ehrenberg, 1872a, p. 314; Sanfilippo et al., 1985, p. 675, fig. 16.6.

Lophocorys biaurita (Ehrenberg) 1875, pl. 10, figs. 7, 8; Bjørklund, 1976, pl. 21, figs. 16, 17.

Lophospyris pentagona (Ehrenberg)1872a, p. 303, pl. 15, fig. 5; Goll, 1976, pp. 398–400, pl. 10, pl. 11, figs. 1–3, 5.

Lophospyris hyperborea Jörgensen, 1905, pp. 130–131, pl. 13, fig. 49, as *Ceratospyris*; Goll, 1976, p. 400, pl. 14, figs. 4–6, 8, 9, 11, 12, pl. 15.

Lychnocanoma nipponica nipponica Sakai, 1980, p. 710, pl. 9, fig. 2a, 2b; Morely and Nigrini, 1995, p. 81, pl. 5, figs. 4, 5.

Lychnocanoma babylonis (Clark and Campbell) 1942, p. 67, pl. 9, figs. 32, 36; Foreman, 1973, p. 437, pl. 2, fig. 1.

Orocena regalis Borgert, 1901, pp. XV 9–10, fig. 8.

Otosphaera polymorpha Haeckel, 1887, p. 116, pl. 7, fig. 6.

Periphaena tripyramis tripyramis (Haeckel) 1887, p. 432, pl. 33, fig. 6; Riedel and Sanfilippo, 1970, p. 521, pl. 4, fig. 8.

Phormocyrtis striata exquisita (Kozlova and Gorbovets) 1966, p. 106, pl. 17, fig. 2; Sanfilippo et al., 1985, p. 678, fig. 20.2.

Phormocyrtis striata striata (Brandt) 1935, p. 55, pl. 9, fig. 12; Sanfilippo et al., 1985; p. 679, fig. 20.1.

Phormocyrtis turgida Krasheninnikov, 1960, p. 301, pl. 3, fig. 17; Sanfilippo et al., 1985, p. 678, fig. 20.5.

Phormospyris stabilis scaphipes (Haeckel) 1887, p. 1033, pl. 84, fig. 13, as *Tristylospyris*; Goll, 1976, p. 394, pl. 8, fig. 9.

Phormostichoartus corbula (Harting) 1863, p. 12, pl. 1, fig. 21; Sanfilippo et al., 1985, p. 703, fig. 34.2.

Phormostichoartus crustula (Caulet) 1979, p. 131, pl. 2, fig. 1; Nigrini and Caulet, 1992, p. 161, pl. 6, figs. 10–14.

Podocyrtis helenae Nigrini, 1974, p. 1070, pl. 1L, figs. 9–11, pl. 4, figs. 4, 5; Sanfilippo et al., 1985, p. 698, fig. 30.13.

Podocyrtis papalis Ehrenberg, 1847, p. 5, fig 2; 1854, pl. 36.23; 1873, p. 251; Riedel and Sanfilippo, 1970, p. 533, pl. 11, fig. 1; Sanfilippo et al., 1985, p. 696, fig. 30.1.

Podocyrtis sp. aff. *Podocyrtis trachodes* Sanfilippo et al., 1985, p. 696, fig. 30.14.

Prunopyle haysi Chen, 1975, p. 454, pl. 9, figs. 3–5; Morley and Nigrini, 1995, p. 82, pl. 2, figs. 1, 4.

Pterocodon lex Sanfilippo and Riedel, 1979, p. 505, pl. 1, figs. 9, 10.

Sethochytris triconiscus Haeckel, 1887, p. 1239, pl. 57, fig. 13; Sanfilippo et al., 1985, p. 680, fig. 22.1.

Sethostylus dentatus Haeckel, 1887, p. 429, pl. 34, fig. 1.

Siphocampe arachnea (Ehrenberg) 1862, p. 299; Nigrini, 1977, pp. 255–256, pl. 3, figs. 7, 8.

Siphocampe acephala (Ehrenberg) 1875, p. 70, pl. 11, fig. 5.

Siphonosphaera socialis Haeckel, 1887, p. 106, pl. 6, figs. 1, 2.

Sphaeropyle langii (Dreyer) 1899, p. 89, fig. 54; Petrushevskaya and Kozlova, 1972, pl. 9, fig. 12.

Spongaster tetras Ehrenberg, 1860, p. 833; 1872b, pl. 6(3), fig. 8; Sanfilippo et al., 1985, p. 661, fig. 9.1.

Spongocore puella Haeckel, 1887, p. 347, pl. 48, fig. 6; Van de Paverd, 1995, p. 149, pl. 40, figs. 1–9.

Spongotractus balbis Sanfilippo and Riedel, 1974, p. 518, pl. 2, figs. 1–3, pl. 25, figs. 1, 2.

Sticholagena? sp. A. Hollis, 2002, p. 311, pl. 8, fig. 16.

Stylacontartium acquilonium (Hays) 1970, p. 214, pl. 1, figs. 4, 5; Kling, 1973, p. 634, pl. 1, figs. 17–20, pl. 14, figs. 1–4.

Stylatractus universus Hays, 1970, p. 215, pl. 1, figs. 1, 2; Morley and Nigrini, 1995, p. 82, pl. 2, fig. 3.

Theocorythium trachelium trachelium (Ehrenberg) 1872a, p. 312; Sanfilippo, et al., 1985, p. 699, fig. 31.1.

Theocorys acroria Foreman, 1973, p. 439, pl. 5, figs. 11–13, pl. 12, fig. 2; Sanfilippo et al., 1985, p. 683, fig. 24.3.

Theocorys anaclasta Riedel and Sanfilippo, 1970, p. 530, pl. 10, figs. 2, 3; Sanfilippo et al., 1985, p. 683, fig. 24.1a–24.1d.

Theocorys anapographa Riedel and Sanfilippo, 1970, p. 530, pl. 10, fig. 4; Sanfilippo et al., 1985, p. 683?, fig. 24.2.

Theocorys (?) *phyzella* Foreman, 1973, p. 440, pl. 5, fig. 8, pl. 12, fig. 1.

Theocotyle ficus (Ehrenberg) 1873, p. 228; 1875, p. 70, pl. 11, fig. 19; Foreman, 1973, p. 441, pl. 4, figs. 16–20.

Theocotyle nigriniae Riedel and Sanfilippo, 1970, p. 525, pl. 6, fig. 5; Sanfilippo et al., 1985, p. 685, fig. 25.1.

Theocotylissa alpha (Foreman) 1973, p. 441, pl. 4, figs. 13–15, pl. 12, fig. 16; Sanfilippo et al., 1985, p. 686, fig. 25.6.

Theocotylissa auctor (Foreman) 1973, p. 441, pl. 4, figs. 8–10, pl. 12, fig. 13; Sanfilippo et al., 1985, p. 686, fig. 25.5.

Tholospyris cortinisca (Haeckel) 1887, p. 1026, pl. 84, fig. 6; Goll, 1969, p. 325, pl. 56, figs. 3, 5, 6, 8.

Tholospyris devexa devexa Goll, 1969, p. 326, pl. 57, figs. 9, 10, 13, 14.

Tholospyris procera Goll, 1969, p. 328, pl. 59, figs. 8, 10–12.

Thyrsocyrtis hirsuta (Krasheninnikov) 1960, p. 300, pl. 3, fig. 16; Sanfilippo et al., 1985, p. 687, fig. 26.2.

Thyrsocyrtis rhizodon Ehrenberg, 1873, p. 262; 1875, p. 94, pl. 12, fig. 1; Foreman, 1973, p. 442, pl. 3, figs. 1, 2.

Tripilidium clavipes Clark and Campbell, 1942, p. 64, pl. 9, fig. 29.

Tristylospyris palmipes Haeckel, 1887, p. 1033, pl. 84, fig. 14; Goll, 1972, p. 969, pl. 83, fig. 2.

Zygocircus productus (Hertwig) 1879, p. 197, pl. 7, fig. 4; Goll, 1979, p. 382, pl. 2, fig. 3.

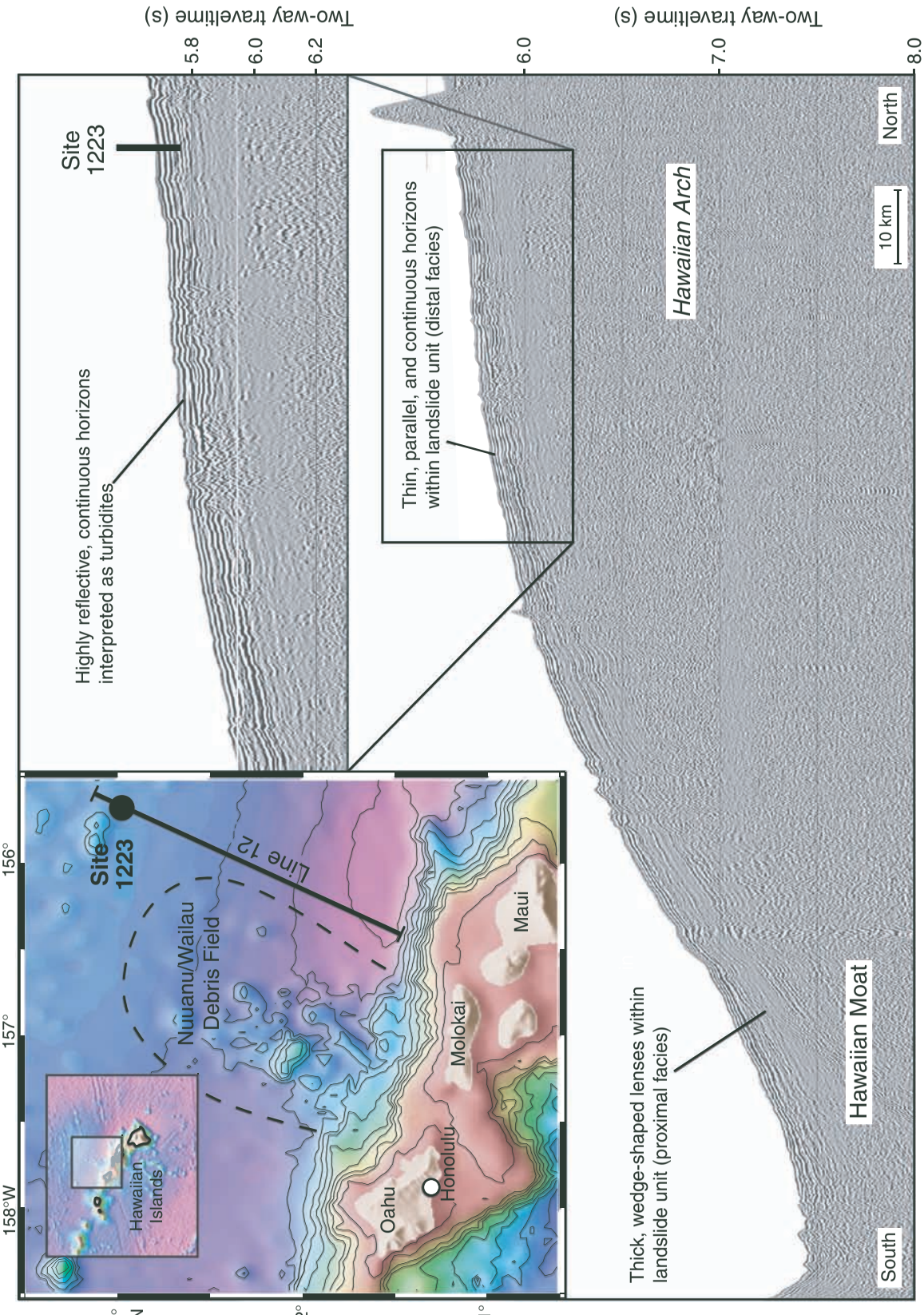

Figure F1. Location of Site 1223 in the central North Pacific Ocean (from Shipboard Scientific Party, 2003, fig. F1).

Figure F2. Distribution of smear slide and strewn slide samples examined for this study and the lithologic units of Shipboard Scientific Party (2003). Radiolaria distribution Intervals A–D, the relative abundance of Radiolaria observed in the smear slides, and the locations of samples reported in Table T2, p. 26, are also displayed. (Continued on next three pages.)

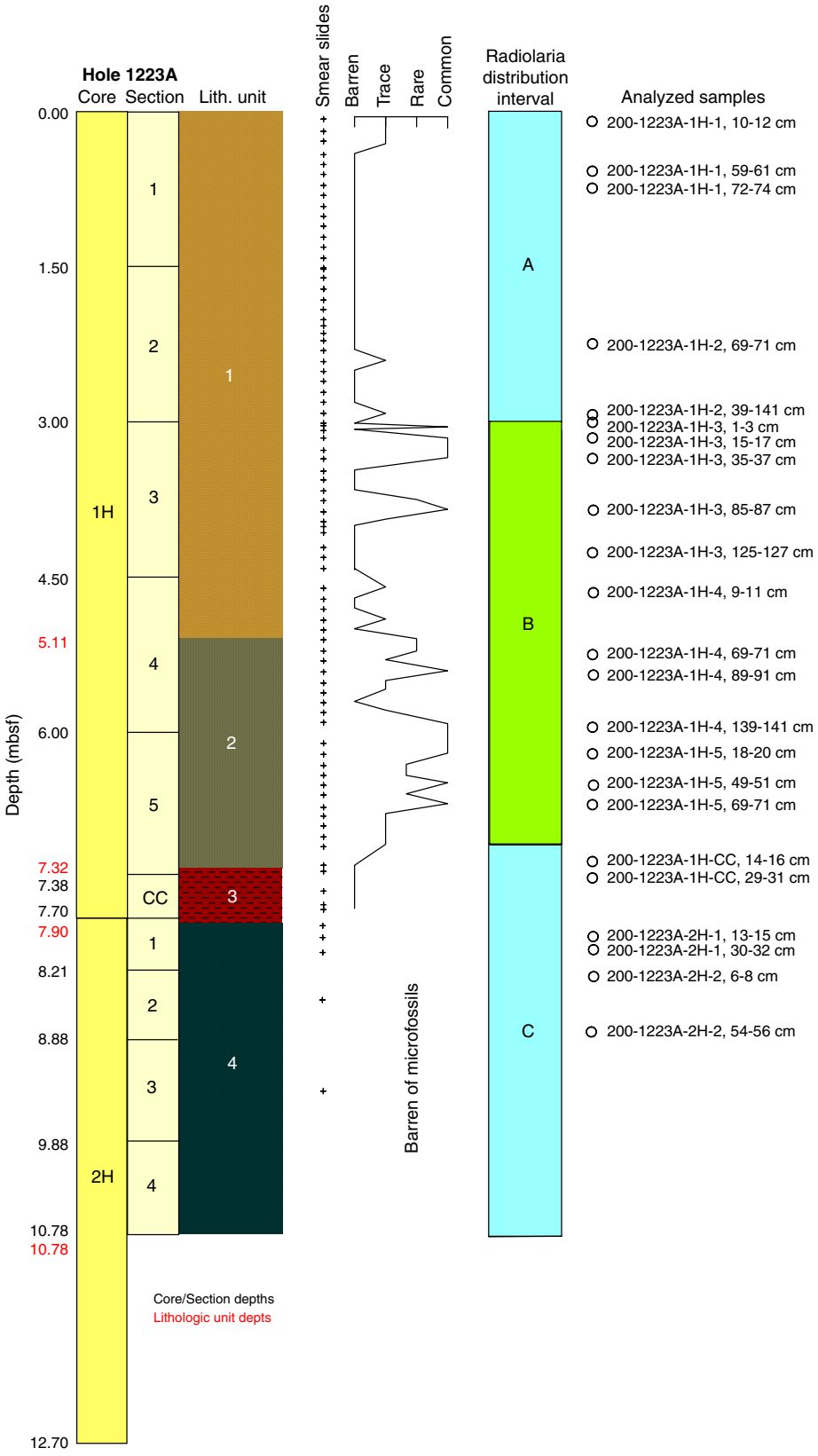

Figure F2 (continued).

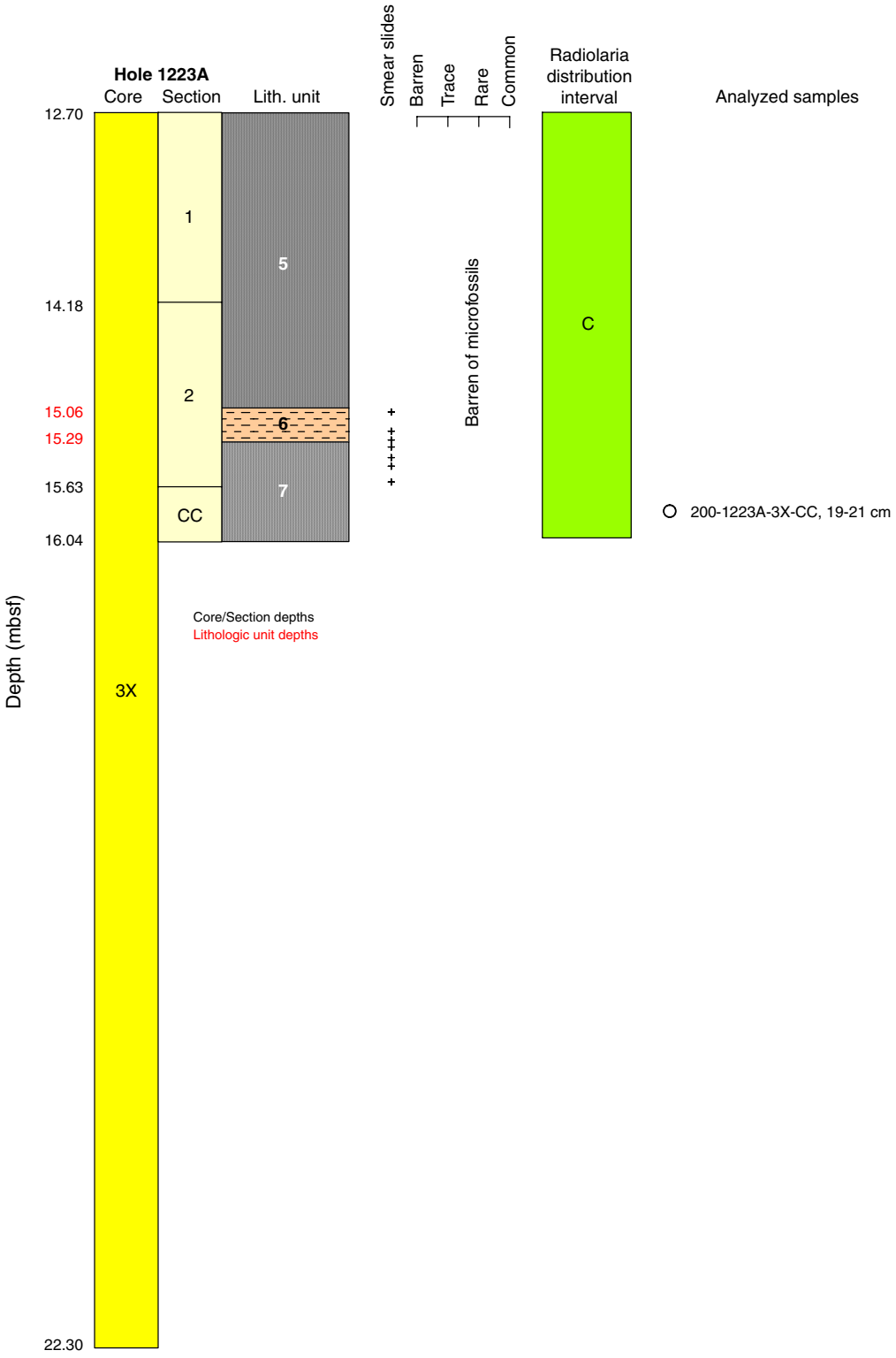

Figure F2 (continued).

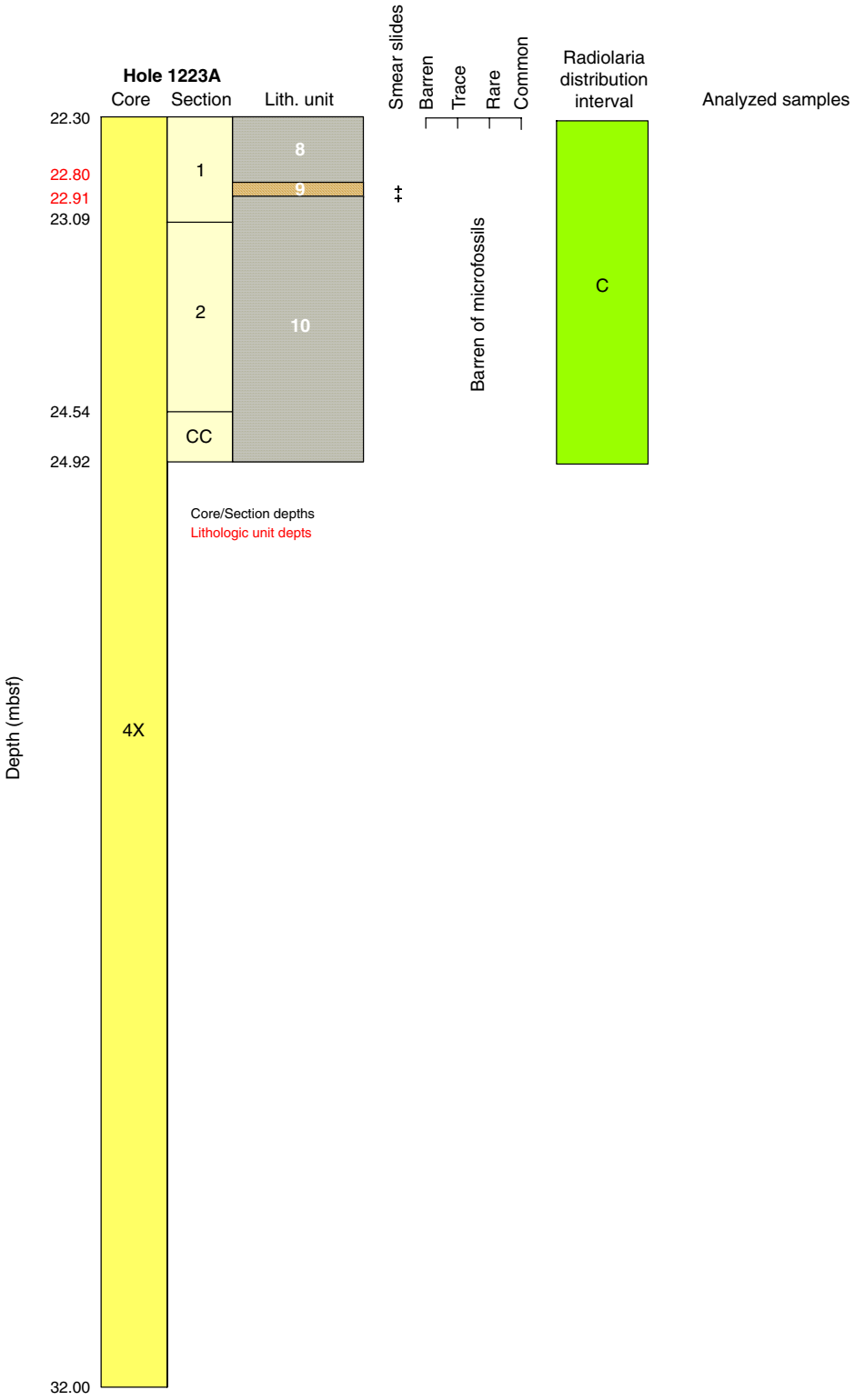

Figure F2 (continued).

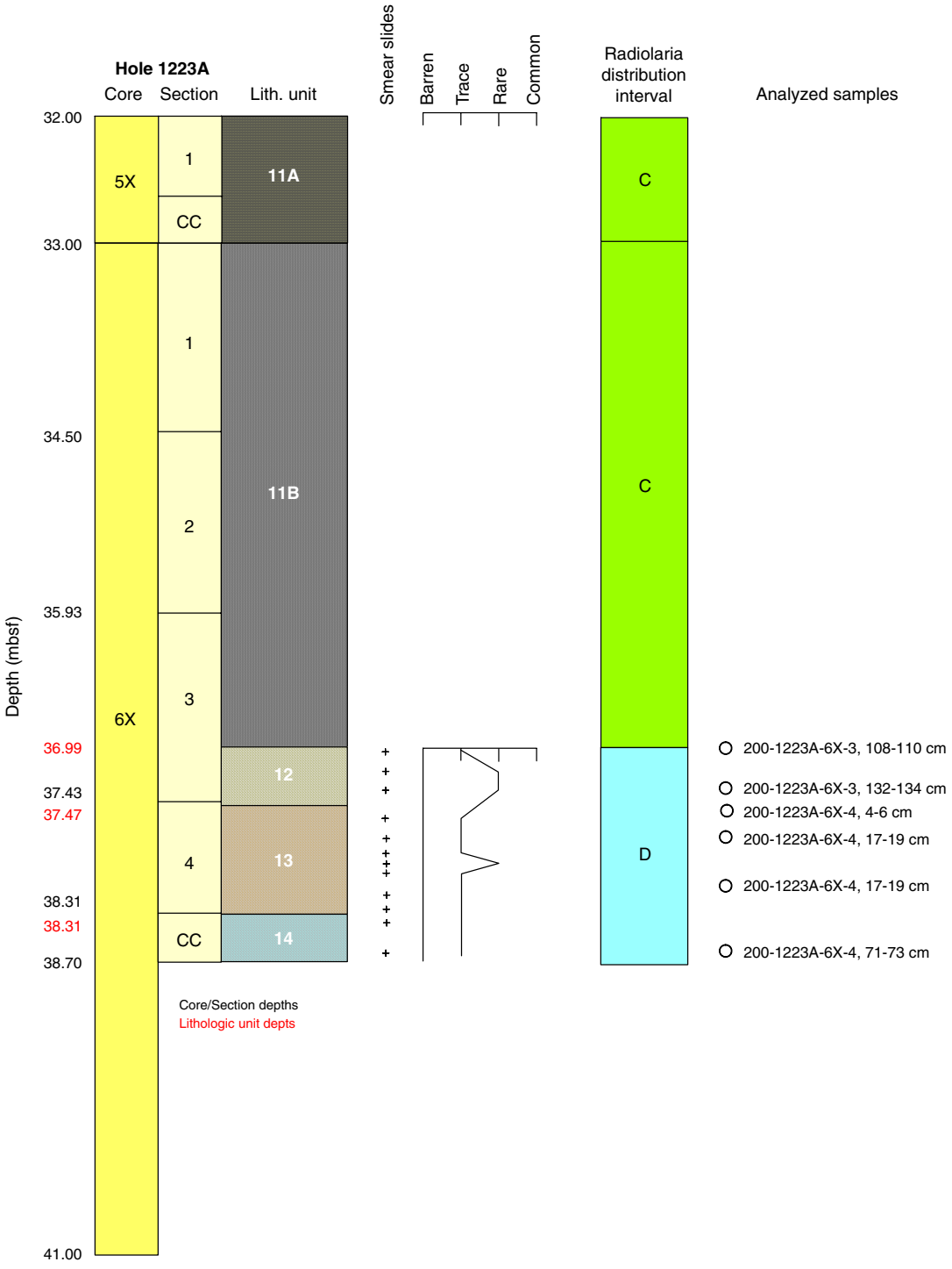

Table T1. Visual descriptions of smear slide samples. (See table notes. Continued on next page.)

Core, section, interval (cm)	Depth (mbsf)	Lithologic unit	Turbidites	Microfossils	Clastic concentration	Radiolarian interval
200-1223A-						
1H-1, 8	0.08	1		No microfossils observed	Low clastics	A
1H-1, 18	0.18			13 radiolarians/cm^2; no other microfossils observed	Low clastics	
1H-1, 29	0.29			13 radiolarians/cm^2; no other microfossils observed	Low clastics	
1H-1, 40	0.4			No microfossils observed	Low clastics	A1
1H-1, 50	0.5			13 radiolarians/cm^2; no other microfossils observed	Low clastics	
1H-1, 60	0.6			13 radiolarians/cm^2; no other microfossils observed	Low clastics	
1H-1, 70	0.7			No microfossils observed	Low clastics	
1H-1, 80	0.8			No microfossils observed	Moderate clastics	
1H-1, 90	0.9		X	No microfossils observed	Moderate clastics	
1H-1, 100	1			No microfossils observed	Very high clastics	
1H-1, 110	1.1			No microfossils observed	Low clastics	
1H-1, 120	1.2			No microfossils observed	Low clastics	
1H-1, 130	1.3			No microfossils observed	Moderate clastics	
1H-1, 140	1.4			No microfossils observed	High clastics	A
1H-1, 150	1.5			No microfossils observed	High clastics	
1H-2, 1	1.51			No microfossils observed	High clastics	
1H-2, 10	1.6			No microfossils observed	Low clastics	
1H-2, 20	1.7			No microfossils observed	Low clastics	
1H-2, 30	1.8			No microfossils observed	Low clastics	
1H-2, 40	1.9			Abundant very fine spiculate crystals; dubious sponge spicules	Moderate clastics	
1H-2, 50	2			Abundant very fine spiculate crystals; dubious sponge spicules	Moderate clastics	
1H-2, 57	2.07			13 radiolarians/cm^2; no other microfossils observed	High clastics	
1H-2, 62	2.12		X	No microfossils observed	Very high clastics	
1H-2, 70	2.2		X	26 radiolarians/cm^2; no other microfossils observed	Very high clastics	A2
1H-2, 80	2.3		X	No microfossils observed	Very high clastics	
1H-2, 90	2.4		X	26 radiolarians/cm^2; no other microfossils observed	Very high clastics	
1H-2, 100	2.5		X	No microfossils observed	Very high clastics	
1H-2, 110	2.6			No microfossils observed	Low clastics	
1H-2, 120	2.7			No microfossils observed	High clastics	A
1H-2, 130	2.8			No microfossils observed	Low clastics	
1H-2, 140	2.9			No microfossils observed	Moderate clastics	
1H-2, 150	3			No microfossils observed	Very high clastics	
1H-3, 2	3.02			52 radiolarians/cm^2; no other microfossils observed	Very high clastics	
1H-3, 8	3.08			184 radiolarians/cm^2; no other microfossils observed	Moderate clastics	
1H-3, 16	3.16			460 radiolarians/cm^2; no other microfossils observed	Low clastics	B1
1H-3, 26	3.26			131 radiolarians/cm^2; no other microfossils observed	Moderate clastics	
1H-3, 36	3.36			65 radiolarians/cm^2; no other microfossils observed	Moderate clastics	
1H-3, 46	3.46			No microfossils observed	Low clastics	
1H-3, 56	3.56			No microfossils observed	Low clastics	B
1H-3, 66	3.66			No microfossils observed	Moderate clastics	
1H-3, 76	3.76		X	40 radiolarians/cm^2; no other microfossils observed	High clastics	
1H-3, 86	3.86		X	65 radiolarians/cm^2; no other microfossils observed	Moderate clastics	B2
1H-3, 96	3.96		X	171 radiolarians/cm^2; no other microfossils observed	Very high clastics	
1H-3, 98	3.98		X	No microfossils observed	Very high clastics	
1H-3, 108	4.08			No microfossils observed	Low clastics	
1H-3, 120	4.2			No microfossils observed	Low clastics	
1H-3, 130	4.3			No microfossils observed	Low clastics	
1H-3, 140	4.4			No microfossils observed	Low clastics	
1H-4, 10	4.6			No microfossils observed	Moderate clastics	B
1H-4, 20	4.7			No microfossils observed	Low clastics	
1H-4, 30	4.8			No microfossils observed	Low clastics	
1H-4, 40	4.9			No microfossils observed	Moderate clastics	
1H-4, 50	5			No microfossils observed	Low clastics	
1H-4, 60	5.1			118 radiolarians/cm^2; no other microfossils observed	Very high clastics	
1H-4, 70	5.2	2	X	26 radiolarians/cm^2; no other microfossils observed	Very high clastics	B3
1H-4, 80	5.3		X	13 radiolarians/cm^2; 1 small foraminifer	Very high clastics	
1H-4, 90	5.4		X	13 radiolarians/cm^2; 1 small foraminifer	Very high clastics	
1H-4, 100	5.5		X	No microfossils observed	Very high clastics	
1H-4, 110	5.6		X	No microfossils observed	Very high clastics	B
1H-4, 120	5.7		X	No microfossils observed	Very high clastics	

Table T1 (continued).

Core, section, interval (cm)	Depth (mbsf)	Lithologic unit	Turbidites	Microfossils	Clastic concentration	Radiolarian interval
1H-4, 130	5.8		X	184 radiolarians/cm^2; no other microfossils observed	Very high clastics	
1H-4, 140	5.9		X	341 radiolarians/cm^2; no other microfossils observed	Very high clastics	
1H-5, 10	6.1		X	709 radiolarians/cm^2; no other microfossils observed	Very high clastics	
1H-5, 20	6.2		X	617 radiolarians/cm^2; no other microfossils observed	Very high clastics	
1H-5, 30	6.3		X	40 radiolarians/cm^2; no other microfossils observed	Very high clastics	
1H-5, 40	6.4		X	13 radiolarians/cm^2; no other microfossils observed	Very high clastics	
1H-5, 50	6.5		X	381 radiolarians/cm^2; no other microfossils observed	Very high clastics	B4
1H-5, 60	6.6		X	118 radiolarians/cm^2; no other microfossils observed	Very high clastics	
1H-5, 70	6.7		X	945 radiolarians/cm^2; no other microfossils observed	Very high clastics	
1H-5, 80	6.8		X	40 radiolarians/cm^2; no other microfossils observed	Very high clastics	
1H-5, 90	6.9		X	26 radiolarians/cm^2; no other microfossils observed	Very high clastics	
1H-5, 100	7		X	13 radiolarians/cm^2; no other microfossils observed	Very high clastics	
1H-5, 110	7.1		X	79 radiolarians/cm^2; no other microfossils observed	Very high clastics	
1H-5, 129	7.29		X	No microfossils observed	Low clastics	
1H-5, 133	7.33	3		No microfossils observed	Clay rich; tabular crystals	
1H-CC, 2	7.52			No microfossils observed	Moderate clastics	
1H-CC, 15	7.65			No microfossils observed	Clay rich; tabular crystals	
1H-CC, 31	7.81			No microfossils observed	Clay rich; tabular crystals	
2H-1, 8	7.78			No microfossils observed	Low clastics	
2H-1, 18	7.88			No microfossils observed	Low clastics	
2H-1, 35	8.05	4		No microfossils observed	Very high clastics	
2H-2, 26	8.47			No microfossils observed	Very high clastics	
2H-3, 50	9.38			No microfossils observed	Very high clastics	
3H-2, 83	15.01	6		No microfossils observed	Low clastics	C
3H-2, 101	15.19			No microfossils observed	High clastics	
3H-2, 108	15.26			No microfossils observed	High clastics	
3H-2, 112	15.3	7		No microfossils observed	Very high clastics	
3H-2, 120	15.38			No microfossils observed	Very high clastics	
3H-2, 128	15.48			No microfossils observed	Very high clastics	
3H-2, 142	15.6			No microfossils observed	High clastics	
4H-1, 54	22.84	9		No microfossils observed	Low clastics	
4H-1, 60	22.9			No microfossils observed	Low clastics	
4H-2, 18	23.23	10		No microfossils observed	Very high clastics	
6H-1, 10	37.03	12		26 radiolarians/cm^2; no other microfossils observed	Low clastics	
6H-4, 14	37.57	13		13 radiolarians/cm^2; no other microfossils observed	Low clastics	
6H-4, 29	37.72			26 radiolarians/cm^2; no other microfossils observed	High clastics	
6H-4, 40	37.83			26 radiolarians/cm^2; no other microfossils observed	High clastics	
6H-4, 51	37.92			52 radiolarians/cm^2; no other microfossils observed	High clastics	
6H-4, 60	38.01			13 radiolarians/cm^2; no other microfossils observed	High clastics	
6H-4, 71	38.72	14		13 radiolarians/cm^2; no other microfossils observed	High clastics	D
6H-4, 84	38.27			26 radiolarians/cm^2; no other microfossils observed	High clastics	
6H-4, 126	38.69			118 radiolarians/cm^2; no other microfossils observed	Clastic rich; tabular crystals	
6H-4, 140	38.83			131 radiolarians/cm^2; no other microfossils observed	Clastic rich; tabular crystals	
6H-CC, 7	38.38			13 radiolarians/cm^2; no other microfossils observed	High clastics	
6H-CC, 33	38.64			13 radiolarians/cm^2; no other microfossils observed	Low clastics	

Notes: Lithologic units from Shipboard Scientific Party (2003). X = samples taken from basal turbidite units.

Table T2. Biostratigraphic distribution of Eocene and Neogene Radiolaria. (This table is available in an **oversized format.**)